



Open Archive Toulouse Archive Ouverte (OATAO)

OATAO is an open access repository that collects the work of Toulouse researchers and makes it freely available over the web where possible.

This is an author-deposited version published in: <http://oatao.univ-toulouse.fr/>
Eprints ID: 6182

To link to this article: DOI:10.1080/01932691.2011.616361
URL: <http://dx.doi.org/10.1080/01932691.2011.616361>

To cite this version: Chabni, Malika and Bougherra, Hadda and Lounici, Hakim and Ahmed-Zaid, Toudert and Canselier, Jean-Paul and Bertrand, Joël (2011) Evaluation of the Physical Stability of Zinc Oxide Suspensions Containing Sodium Poly-(acrylate) and Sodium Dodecylsulfate. *Journal of Dispersion Science and Technology* vol. 32 (n°12). pp. 1786-1798. ISSN 0193-2691

Any correspondence concerning this service should be sent to the repository administrator: staff-oatao@listes-diff.inp-toulouse.fr

Evaluation of the Physical Stability of Zinc Oxide Suspensions Containing Sodium Poly-(acrylate) and Sodium Dodecylsulfate

Malika Chabni,¹ Hadda Bougherra,² Hakim Lounici,¹ Toudert Ahmed-Zaïd,² Jean-Paul Canselier,³ and Joël Bertrand³

¹Faculté des Sciences, Département de Chimie, Université M. Mammeri, Tizi-Ouzou, Algeria

²Département de Génie Chimique, Ecole Nationale Polytechnique, Ave Pasteur, Hassen Badi, El-Harrach—Algiers, Algeria

³Université de Toulouse, Laboratoire de Génie Chimique, ENSIACET/INPToulouse, France

The physical stability of zinc oxide (ZnO) aqueous suspensions has been monitored during two months by different methods of investigation. The suspensions were formulated with ZnO at a fixed concentration (5 wt%), sodium poly-(acrylate), as a viscosifier, and sodium dodecylsulfate (SDS), as a wetting agent. The rheological study shows that the suspensions exhibit a non-Newtonian, most often shear-thinning behavior and their apparent viscosity increases with polymer concentration. The rheograms of most of the ZnO suspensions do not vary during the experimental period. The viscoelastic properties of these suspensions, such as elastic or storage modulus (G'), viscous or loss modulus (G'') and phase angle (δ) were also examined. For % strains lower than 10%, all the formulations show strong elastic properties ($G' > G''$, δ varies between 5 and 15°). Beyond 10% strain, the rheological behavior changes progressively from elastic to viscous ($G'' > G'$ for % strain >80%). Consistently, δ increases and reaches the 50–70° zone.

Multiple light scattering (back-scattered intensity), measured with the Turbiscan ags, was used to characterize suspension physical stability (early detection of particle or aggregate size variations and particle/aggregate migration phenomena). Suspensions containing 0.4 and 0.6 wt% polymer remain stable and macroscopically homogeneous, without being affected by the change of particle size observed with a laser particle sizer. Sedimentation tests, pH, and ζ potential measurements versus time, also confirmed these findings.

Keywords ζ potential, sodium poly-(acrylate), multiple light scattering, particle size distribution, rheology, sodium dodecylsulfate, ZnO suspension

INTRODUCTION

In pharmaceutical suspensions, when a solid active ingredient is dispersed in a liquid, the problems are related to agglomeration, flocculation (increase of particle size) and sedimentation: because of their high surface area, micro- or nanoparticles form aggregates or agglomerates due to Van der Waals or other attractive forces.

The control of colloidal properties and long-term stability of the dispersion of solid active particles is of significant importance in the manufacture of high quality products. The formulation of pharmaceutical suspensions requires that sedimentation is minimized.

Many investigations are concerned by understanding the effects of organic additives, such as polymers, on the stability of colloidal suspensions. Polymer chains adsorb onto particle surface that they tend to stabilize. This phenomenon is accompanied with changes in the microstructure of the solid particles.^[1–12]

Polymer adsorption serves as an effective way for modifying particle surface and hence improving the stability of pharmaceutical suspensions against flocculation. The adsorption of polymeric additives onto the surface of the solid active ingredient is the result of particle-particle interactions: hydrogen bonding and Van Der Waals forces. Therefore, the mechanism of polymer adsorption and its effect on the stability of dispersions are important in controlling suspension properties. When adsorbed on inorganic surfaces, these species impart electrostatic, steric or electrosteric stabilization.

A lot of pharmaceutical suspensions contain carbomers (synthetic polymers, e.g., poly-(acrylic acid), crosslinked

Address correspondence to Jean-Paul Canselier, Université de Toulouse, Laboratoire de Génie Chimique, ENSIACET/INPToulouse, 4 allée Emile Monso, BP84234, 31432 Toulouse Cedex 4, France. E-mail: jeanpaul.canselier@ensiacet.fr

polyacrylates) as viscosifiers. Only small amounts of carbomer are needed to bring the viscosity of an aqueous preparation to almost any desired value. Pharmaceutical suspensions have a maximum stability in a certain pH range: in fact, the pH of the medium has a great influence on the viscosity of the carbomer solution, therefore on suspension stability.^[13] For unneutralized dispersions of carbomer, pH values range between 2.5 and 3.5, depending on polymer concentration. Neutralized aqueous carbomer gels are more viscous at pH 6–11. Viscosity is considerably reduced for pH less than 3 or greater than 12. Viscosity is also reduced in the presence of strong electrolytes.^[14] It is significant to check that the pH of these suspensions remains in a range corresponding to high polymer viscosity. Thus, pH measurements allow good control of the manufacturing process.

Polymers and surfactants are used together in several applications. As a result, interactions between polymers and charged surfactants in aqueous solutions have attracted increasing attention because of their complex behaviors and potential applications in rheological control, detergency, and pharmaceutical formulations.^[15] Yet, there are very few investigations on the interactions between carboxylates, such as poly-(acrylic) acid (PAA), and anionic surfactants, such as sodium dodecylsulfate (SDS). Using fluorescence, conductivity and viscosity measurements, Binana-Limbele and Zana^[16] and Iliopoulos et al.^[17] concluded that there was no direct interaction between SDS and NaPAA. However, obviously, as a sodium salt, the latter decreases the critical micelle concentration (CMC) of SDS through electrostatic effects. On the other hand, Maltesh and Somasundaran^[18] reported that, in an earlier study, Eliassaf had observed that, at low values of pH, the reduced viscosity of PAA increased as SDS concentration was increased. Through a fluorescence spectroscopic investigation, Maltesh and Somasundaran^[18] found that these interactions depended significantly on PAA concentration and pH (ionization degree of PAA). Wang and Tam^[19] also reported evidence of interaction between SDS and PAA for a neutralization degree of PAA lower than 0.2. Hydrocarbon chains of SDS cooperatively bind to apolar segments of PAA through hydrophobic interaction.

Zinc oxide (ZnO) has generated considerable attention because of its optical, magnetic, antibacterial and semiconducting properties.^[1–5] Its nanostructures exhibit interesting properties: high catalytic efficiency and strong adsorption capacity, and it is extensively used in many applications such as cosmetics, paints, ceramics and electronics. In most of these applications, a highly stable dispersion is required.

The aim of the present study was to investigate the effects of PAA and sodium dodecylsulfate (SDS), used as a wetting agent, on the stability of pharmaceutical suspensions containing 5 wt% ZnO. The physical stability of these

suspensions has been monitored, during two months, by different experimental techniques: rheology, with a controlled stress rheometer, particle size distribution (PSD), multiple light scattering, ζ potential, sedimentation rate, and pH measurements. The influence of the ingredients on the stability of ZnO suspensions has been investigated as well as the nature of particle-particle and particle-additive interactions.

EXPERIMENTAL

Materials

All of the chemicals used in this study were of analytical reagent grade (Table 1).

Methods

Preparation of Formulations

The ZnO suspensions were prepared in a stirred tank equipped with a Rushton turbine and four baffles: this device operates in a mixed flow regime (between axial and radial types).

Polyacrylic acid was first dispersed in water. A sufficient quantity of 0.1 N NaOH was added to neutralize the polyacrylic acid, stirring gently to avoid formation of air bubbles. In order to achieve maximum viscosity, 1 g carbomer was neutralized with approximately 0.4 g NaOH. ZnO and SDS were then added while mixing until homogeneous. The compositions of the suspensions studied are given in Table 2.

Evaluation of the Physical Stability of Formulations

In order to evaluate the physical stability of the suspensions, a few physical characteristics, among those susceptible to change during storage, have been measured at regular time intervals.

pH measurements. The pH measurements were performed using a MP220 model (Mettler Toledo) pHmeter.

Rheological characterization. The rheological characterization of ZnO suspensions and sodium polyacrylate

TABLE 1
Ingredients of the formulated suspensions

Compound	Formula, composition, manufacturer
Zinc oxide	ZnO, purity 99% min. Prolabo
Sodium dodecylsulfate (SDS)	C ₁₂ H ₂₅ SO ₄ ⁻ Na ⁺ , 99% min. Merck
Polyacrylic acid (PAA)	[-CH ₂ -CH(COOH) ⁻] _n (M ≈ 1250000). Aldrich
Sodium hydroxide	NaOH
Distilled water	

TABLE 2
Composition of the suspensions
(all containing 5 wt% ZnO)

No.	Polymer (polyacrylic acid)	Sodium dodecylsulfate
F1	0.20	0.50
F2	0.20	1.50
F3	0.60	0.50
F4	0.60	1.50
F5	0.12	1.00
F6	0.68	1.00
F7	0.40	0.29
F8	0.40	1.71
F9	0.40	1.00

solutions was performed using an AR2000 rheometer (TA Instruments), equipped with cone-plane geometry of 2° angle and 60 mm diameter. The plate was fixed. The shearing torque, imposed on the measurement tool, was transmitted to the sample, whose flow caused the rotation of the tool, and speed measurement. Since, during sampling, the state of the sample was likely to undergo some structural modification, the sample was left at rest in the apparatus during 10 minutes before measurement, so that it could recover its initial state.

To determine the linear viscoelastic domain and study the viscoelastic properties of the suspensions, oscillation tests were carried out ($f = 1$ Hz, $t = 25^\circ\text{C}$).

Particle size. The suspensions were characterized with a laser particle sizer (Master Sizer 2000, Malvern, UK). They were first diluted, then put into circulation in a suitable cell. The particles, illuminated by a He/Ne laser, deflect light from its principal axis. The quantity of light deflected and the value of the deviation angle can measure particle size precisely. Measurable diameters range from 0.02 to 2000 μm .

Analysis with the Turbiscan. The Turbiscan ags (Formulation, France) is an optical apparatus whose main purpose is to characterize concentrated dispersions. The sample is contained in a cylindrical measuring glass cell, 55 mm high, closed with a waterproof stopper. The light source is a diode emitting in the near infrared ($\lambda = 880$ nm). Two synchronous optical detectors receive the light transmitted through the sample (180° from the incident light, transmission detector), and the light backscattered by the sample (45° from the incident light, backscattering detector). The optical source scans the whole sample, acquiring transmission and backscattering intensity data every 40 μm . The time interval between two successive acquisitions is programmed by the user, two analyses per day in the case of our formulations. This mode is the most comprehensive analysis to detect migration phenomena [20].

ζ Potential measurements. The ζ potential measurements were performed with a ZetaNano Z (Malvern Instruments). A laser beam passes through the sample, which must be optically clear. It is thus necessary to filter or to centrifuge the primary sample to recover the supernatant, containing the finest particles.

Sedimentation/clarification rate. The sedimentation rate of a suspension, F , was deduced from the time variation of the height of the sediment, H_s , compared with the total height, H_t : $F = 100 H_s/H_t$.

Our suspensions being opaque, it was difficult to measure the height of the sediment. Therefore, the clarification rate of the suspensions was deduced from the variation of the height of the transparent part, H_c , versus time ($100 H_c/H_t$).

RESULTS AND DISCUSSION

pH Measurements

Some suspensions show a maximum stability in a certain pH range. Any pH shift of this parameter causes a change in rheological properties that may adversely affect suspension stability.

The evolution of pH of the different formulations versus time is illustrated in Figure 1.

Figure 1 shows that the initial pH of our suspensions ranges between 8 and 9, because of neutralization with concentrated NaOH and does not vary significantly versus time. It remains in the range of 6 to 11 corresponding to the maximum viscosity of polymer solutions, thus to good suspension stability. This allows to say that the impact of pH on the destabilization observed in some formulations is negligible.

Rheological Studies

The rheological characterization of zinc oxide-additive mixtures aims at a better understanding of the interactions

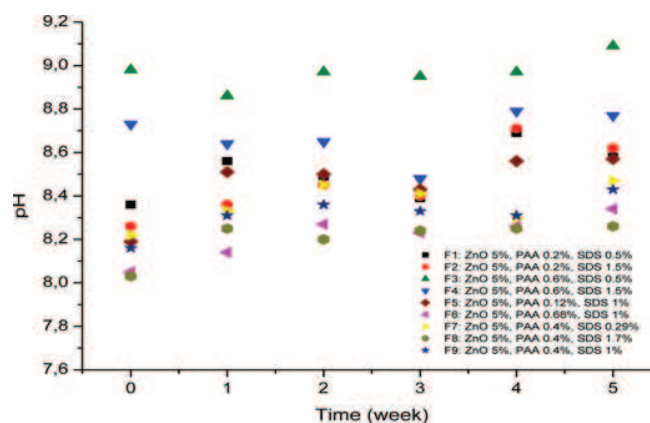


FIG. 1. Evolution of pH for the different formulations as a function of time. (Color figure available online.)

between zinc oxide particles and between the additive components, i.e., between polymer and surfactant.

Viscoelasticity: Dynamic Mechanical Tests

Particle-particle interactions contribute remarkably to the macroscopic response of a system. To understand the structure responsible for the observed rheological behavior, dynamic rheometry (strain sweep) was used. The formulations were studied under conditions close to the rest, without rupture of the internal structure.

Strain sweep. The graphs of Figure 2, originating from oscillation tests, illustrate typical strain sweep profiles, showing the change of the oscillation stress and the G' and G'' moduli, as a function of the percentage of strain, for the formulations with various additive concentrations.

Figure 2a shows that all the formulations present a linear behavior for the lower deformations (less than 1% strain). In this region, the response (oscillation stress) at any time is directly proportional to the strain. The end of the linear viscoelastic domain indicates a «yield stress» corresponding to a “critical strain”; a value beyond which there will be a modification of the structure of the sample, which begins to flow.^[21]

Comparing the formulation F1 (0.2% strain, 3.4 Pa of stress) with F3 (0.7%, 4 Pa), F2 (0.4%, 6.6 Pa) with F4 (0.4%, 173.8 Pa), F5 (0.3%, 18.2 Pa) with F6 (0.5%, 97.7 Pa) and F9 (0.6%, 8 Pa) with F6 (0.5%, 97.7 Pa), we see that, for the same surfactant content, the “critical strain” increases with polymer concentration (Figures 2a1 and 2a2).

Similarly, a comparison of the formulations F1 (0.2%, 3.4 Pa) and F2 (0.4%, 6.6 Pa), F3 (0.7%, 4 Pa) and F4 (0.4%, 173.8 Pa), and F7 (0.2%, 3.3 Pa), F8 (0.3%, 37 Pa) and F9 (0.6%, 8 Pa), shows that, for the same polymer content, the “critical strain” increases with surfactant concentration (Figures 2a1 and 2a3).

The frontier between solid and liquid states is not very clear. Some substances show an intermediate behavior between that of a perfect elastic solid and that of a Newtonian viscous liquid, such as viscoelastic materials. For a better understanding of the viscoelastic behavior of our formulations, the results of strain sweep are given in terms of G' (elastic or storage modulus) and G'' (viscous or loss modulus) as a function of % strain in Figure 2b.

For deformations lower than 10⁻²% (at rest), the elastic modulus, G' , for all formulations, is much higher than G'' , indicating a strong thickening or solidifying behavior.^[21,22] In the linear domain, G' remains unchanged while G'' increases with the deformation, decreasing the $G'-G''$ gaps. That indicates a predominance of the viscous behavior.

Once the critical strain is reached (around 1% strain), the $G'-G''$ gap reaches its minimal value. Beyond this strain, G' starts to decrease simultaneously with G'' and the $G'-G''$ gap is maintained practically constant, meaning

that the overall viscoelastic behavior of our formulations remains unchanged within this range of deformations.

At about 10% strain, G'' increases again for F3 and F4 formulations, while G' continues to decrease, thus narrowing the $G'-G''$ gap. This indicates the transition from an elastic to a viscous behavior (change of structure of the formulations, and hence, of their flow characteristics).^[21,22] We suppose that this transition, at low deformations, is an interesting and desirable characteristic since it simulates the onset, so the facility, of spreading of formulations on the skin. Consequently, the knowledge of these viscoelastic parameters is a first approach to predict the performance of the products.^[22]

When the deformation reaches 30%, for F1, F6, and F7, G' sharply decreases while G'' increases. It is likely that the sample slipped or was ejected from the gap between cone and plate. For these formulations, it would have been necessary to use a sanded or striated surface.

At about 80% strain, for F3 and F4, the G' and G'' cross each other, meaning a true viscoelastic behavior. We can suppose that, in this domain of strong deformations (LAOS = Large Amplitude Oscillation Strain), the structure of the product is completely broken.^[21]

Let us note that, in the linear viscoelastic domain, G' and G'' are very sensitive to additive concentrations. PAA and SDS act on the elastic and viscous properties of all the suspensions studied.

The phase angle δ ($\tan \delta = G''/G'$) is a good indicator of the overall viscoelastic nature of the suspensions. Figure 3 shows the variation of δ as a function of percentage of strain, for all formulations.

It has been established that: $\tan \delta < 1$ indicates highly associated particles, $1 < \tan \delta < 3$ weakly associated particles and $\tan \delta$ higher than 3 nonassociated ones.^[23]

At about 0.01% strain (at rest), the phase angle δ is close to 5° for all formulations ($\tan \delta < 1$, highly associated particles). Between 0.01% and 1% strain, δ varies between 5 and 15° ($\tan \delta < 1$, associated particles). Up to 10% strain, δ remains practically unchanged, indicating that the overall viscoelastic structure of the formulations does not change in this region.

Beyond 10% strain, for F3 and F4, δ increases rapidly (change of structure) and, around 80%, reaches 45° ($\tan \delta = G''/G' = 1$), G' and G'' curves cross each other (Figure 2b), meaning a true viscoelastic behavior.

For the other formulations, the increase occurs toward 30% of deformation: for F1, F6, and F7, δ culminates in the 55–65° zone ($1 < \tan \delta < 3$, weakly associated particles), whereas for F2, F5, F8, and F9, δ is found in the 30–35° region ($\tan \delta < 1$, associated particles during the entire test, no crossing of G' and G'' curves) (Figure 2b).

These δ values range between 0° (ideal elastic solid) and 90° (only viscous liquid), indicating that the formulations are viscous enough to allow their spreading on the skin.

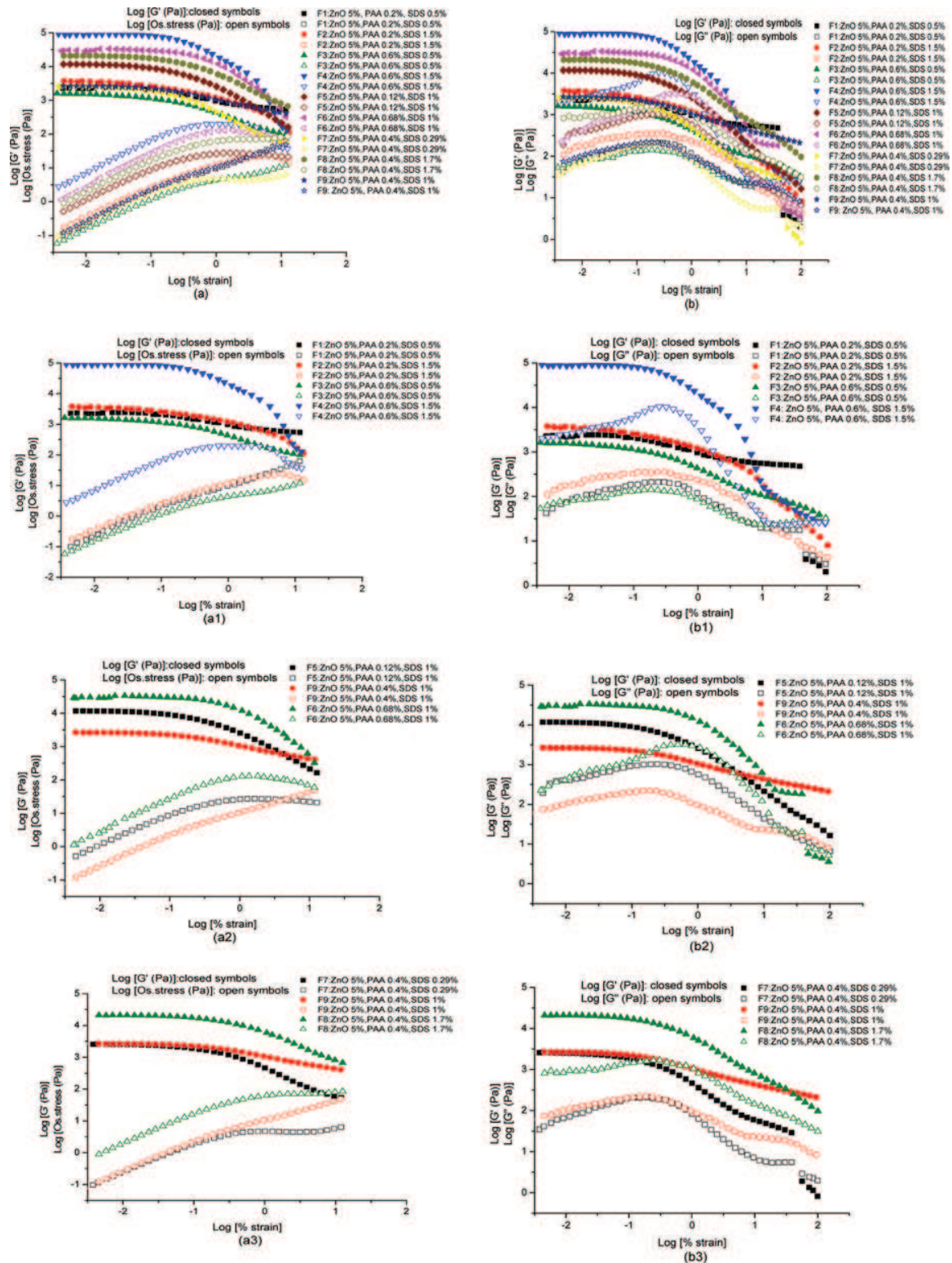


FIG. 2. Typical strain sweep profiles for different formulations. (a) determination of the linear viscoelastic domain: effect of PAA (a1), (a2) and SDS concentrations (a1), (a3). (b) viscoelastic properties (G' and G''): effect of PAA (b1), (b2) and SDS concentrations (b1), (b3). (Color figure available online.)

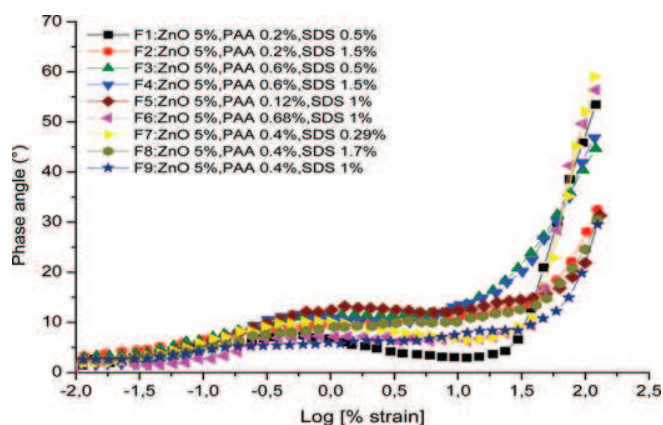


FIG. 3. Variation of the phase angle (δ) as a function of % strain for the different formulations. (Color figure available online.)

Flow Tests

The flow curves for the solutions of sodium polyacrylate and the various formulations are shown in Figures 4a–4f. These curves were obtained using a “steady state flow” procedure.

The rheological behavior of the sodium polyacrylate solutions is very sensitive to the concentration; the shear stress is proportional to polymer concentration. However, for the solution with 0.68% PAA, we observe a change of tendency (Figures 4a–4c). For shear rates lower than 10^{-3} s^{-1} , the 0.12% PAA solution presents a shear-thickening behavior followed by a shear-thinning behavior. However, for the more concentrated solutions, we observe a shear-thinning behavior for all shear rates.

Generally, for concentrated polymer solutions, a shear rate increase modifies the arrangement of the molecules in the medium. At lower shear rates (rest state), polymer chains are very entangled, which confers high viscosity to the solution. An increase of the shear rate allows the stretching of the chains and their arrangement in parallel layers. This makes slipping of polymeric chains easier, thus reducing viscosity (shear-thinning behavior).^[24–26]

Generally, the viscosity of the mixtures increases with the concentration of suspended matter^[21] When additive (polymer and surfactant) concentration is low, the rheological behavior of the suspension is similar to that of the dispersing medium (Newtonian behavior).^[27] This explains the behavior of F1 (ZnO 5%, PAA 0.2%, SDS 0.5%).

The shape of the rheograms is typical of a shear-thinning behavior (Figures 4d–4f). When the shear rate is increased, the molecules or the structural units line up gradually in the direction of the flow. Another molecular interpretation consists to envisage a modification of structure of liquid (destruction by rupture of bonds or deflocculation of particles) with an increase of the shear rate.^[24–26]

The SDS concentration being kept constant, an increase of the PAA concentration causes an increase of the shear stress, therefore of viscosity. In fact, it reinforces chain entanglement and obstructs fluid flow. The effect of SDS concentration on the rheological behavior of the suspensions is less important. Here again, we observe a change of tendency for the F6 formulation. Although its polymer content is higher, it is less viscous than F3 and F4.

In the present study, the surfactant, supposed to play the role of wetting agent, was used at relatively high concentrations in certain formulations. In F8, containing 1.7% SDS, two sharp changes of slope express a suspension destabilization (with possible sedimentation: Figures 4d–4f), showing the acceptable limit of SDS content. This can be explained in terms of competitive adsorption between surfactant and polymer on particle surface.

The flow behavior of our suspensions was investigated as a function of time. The rheograms of F3, compared with those of the polymer solution containing 0.6% PAA, are given on Figures 5a and 5b.

The rheograms of the 0.6% PAA solution are reproducible during all the period of storage and over the whole shear rate range studied. For the F3 formulation, a slight difference between the rheograms of the first two weeks is observed. After 15 days of storage, the difference becomes negligible and the reproducibility of the rheograms is remarkable, especially for shear rates higher than 10^{-2} s^{-1} , indicating an equilibrated balance of the rheological behavior, also observed for other formulations and a good shelf stability of F3.

Particle Size

Figure 6 shows a typical particle size distribution (PSD) measured, after 5 days of storage, by the light scattering technique with the MasterSizer 2000 in dry medium for the ZnO powder and in dilute medium for the “pure” suspension (5% ZnO) and the various formulations.

The PSD are bimodal for the ZnO powder and the “pure” ZnO suspension. The powder presents two populations of particles: a first one, constituted by primary particles, showing a maximum at $0.54 \mu\text{m}$, and a second one at $3.31 \mu\text{m}$, which indicates significant aggregates. This pattern is also observed for the suspension, which clearly reveals two populations: a first one, with a maximum located at $3.34 \mu\text{m}$, and a second population of aggregates, larger than those observed in the ZnO powder, around $182 \mu\text{m}$ (effect of the hydration). The F1 to F9 formulations show monomodal distributions, except F3 and F4, which present a shoulder, between 1 and $3 \mu\text{m}$, indicating the presence of small particles of the same size as those observed in the ZnO powder and the “pure” suspension. For the formulations, the maxima extend from 40 to $80 \mu\text{m}$, meaning that the addition of PAA and SDS causes an increase of the number of smaller particles and reduces

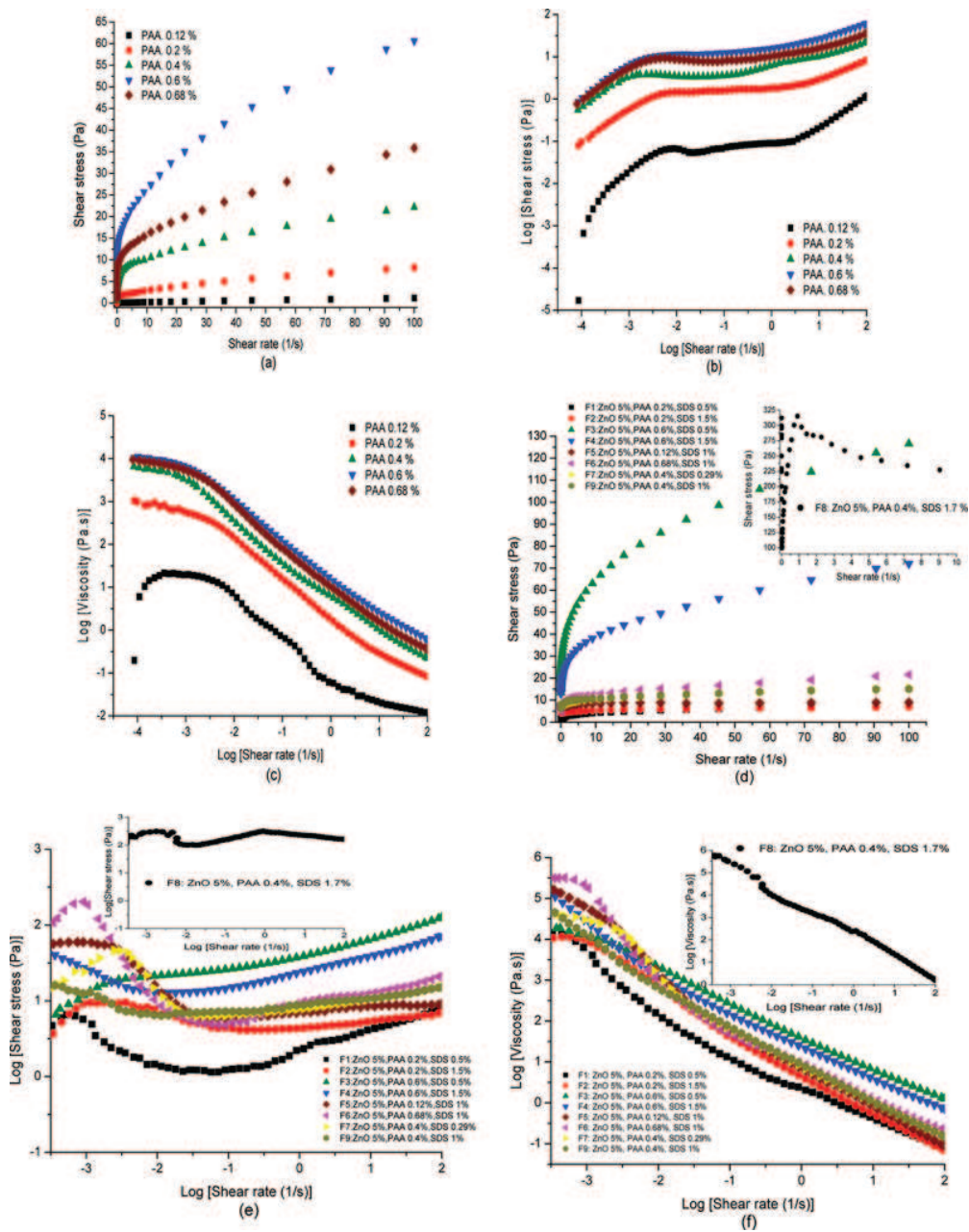


FIG. 4. Flow curves after 5 days of storage, of: (a), (b), and (c) sodium polyacrylate solutions; (d), (e), and (f) the different formulations. (Color figure available online.)

the percentage of larger particles, present in the “pure” suspension. We can interpret this result by the small chains of PAA, which overlap less after neutralization and are less prone to ensure bridging bonds between suspended ZnO particles.

Generally, as for emulsions, the viscosity of the suspensions increases with the decrease of the particle size, which seems well confirmed by our experimental results. The

comparison of the curves shows that the increase of the PAA concentration, at a fixed SDS content, causes a shift toward smaller diameters (Figure 6b). From Figure 6c, we also note that particle size is reduced with an increase of the SDS content, provided that the latter is not too high (change of tendency for 1.7% SDS).

The PSD for the different formulations, after 5 weeks of storage, are illustrated in Figure 7.

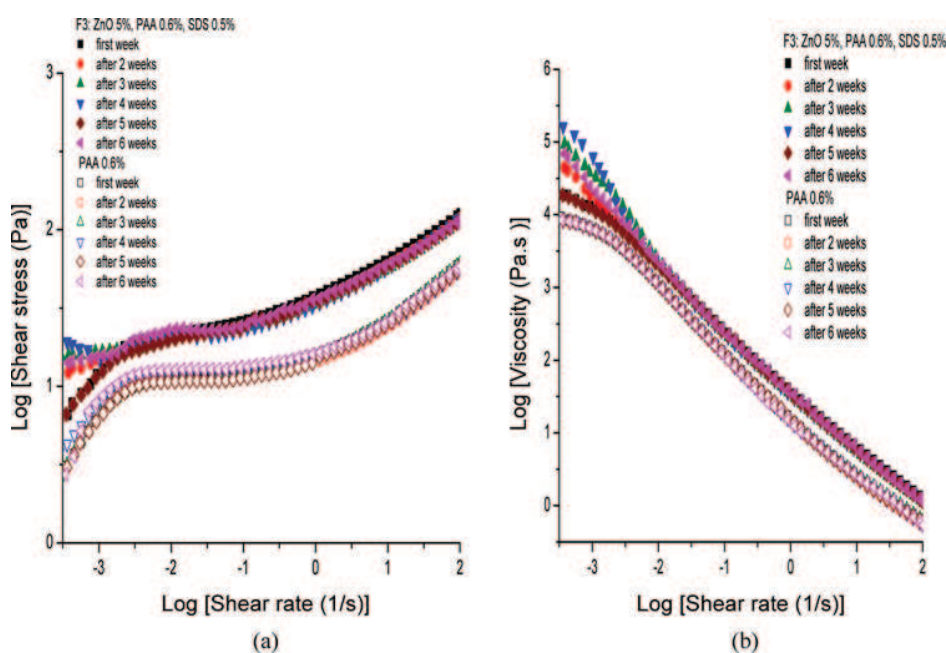


FIG. 5. Flow curves, as a function of time, for F3 and the 0.6% PAA solution: (a) stress versus shear rate (b) viscosity versus shear rate. (Color figure available online.)

Except for F6, the PSD remain monomodal and the maxima undergo slight shifts toward larger diameters. The curves of F7 and F9 show a shoulder around 300 μm , indicating the formation of large aggregates, more significant in volume for F7. The shoulder of the F4 curve, initially observed between 1 and 3 μm , increases in volume, meaning an increase of the number of smaller particles: this could be interpreted by a late manifestation of the effect of the additives.

Figures 7b and 7c show the evolution of the particle size for F3, the most stable formulation, and for F6, which reveals a second population of particles, after three weeks of storage, likely to be due to the formation of large aggregates with a shift of this peak toward larger sizes. Therefore, the suspended particles are of two types: a first population of primary particles and a second population of large aggregates (with diameter reaching 300 μm after 5 weeks of storage).

Multiple Light Scattering Analysis: Turbiscan ags

Particle migration was characterized with the Turbiscan ags during two months. The suspensions are opaque, so we will be interested by the variations of the profiles of backscattering intensity (%) as a function of the height of the sample and of the time of storage in the apparatus (Figures 8a–8i) to detect incipient instabilities. The time-dependent behavior of the backscattering intensity is related to the local variations of particle concentration

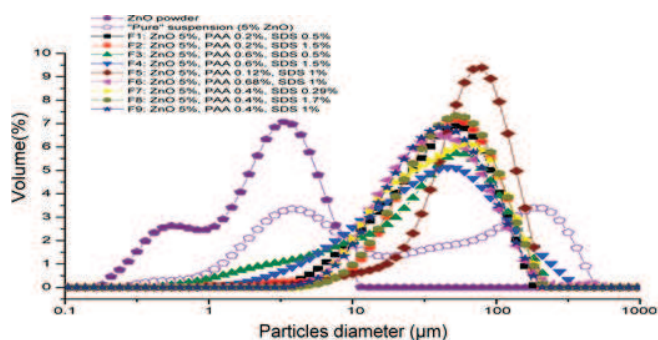
(sedimentation-clarification) and to changes occurring in the inner structure of the suspension (namely particle size) due to particle-particle interaction forces like Van Der Waals' ones, responsible for the formation of flocs and aggregates (flocculation, coagulation).

For F3, F4, and F9, the profile remains uniform and invariant versus time all along the sample. These formulations, containing 0.4 and 0.6 wt% polymer, remain stable and homogeneous. Their homogeneity is not affected by the changes of particle size observed by the laser particle sizer.

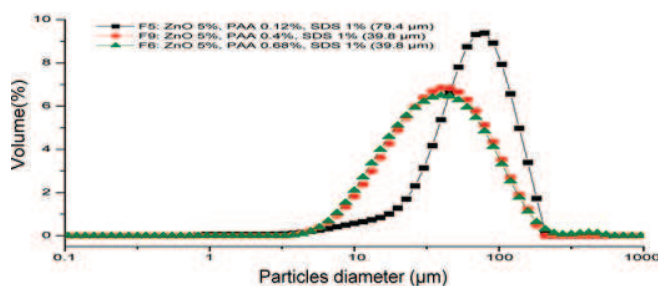
For F1, F2, F5, F7, and F8, we observe local variations related to migratory phenomena. The backscattered intensity increases at the bottom of the sample and decreases in its higher part. This increase of the backscattering intensity corresponds to a local increase of particle concentration (sedimentation). This is justified by the evolution of the PSD, relatively negligible.

For F6, a decrease of the backscattered intensity, versus time all along the sample, corresponds to an increase of particle size, at a given concentration. The time-dependent behavior of the backscattering intensity (increase of the particles size) is due to particle-particle interaction forces like van de Waals' ones, responsible for the formation of flocs and aggregates by flocculation and coagulation. The destabilization of this formulation has also been observed with the laser particle sizer.

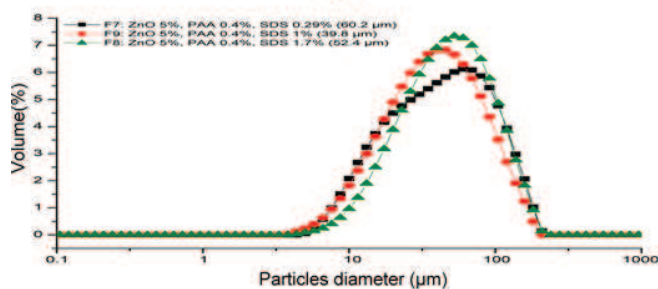
To get a more precise insight of the destabilization phenomena, comparisons of profiles were made, at two



(a)



(b)



(c)

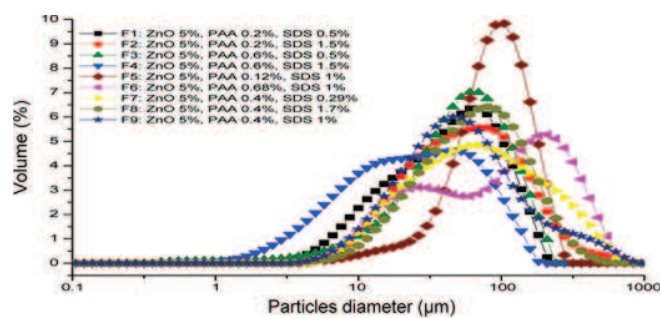
FIG. 6. Particle size distribution for the ZnO powder, the “pure” suspension (5% ZnO) and the various formulations, after 5 days of storage (a). Effect of PAA (b), and SDS (c) contents on particle size. (Color figure available online.)

weeks of interval, for each formulation. The results are illustrated by Figures 9a–i.

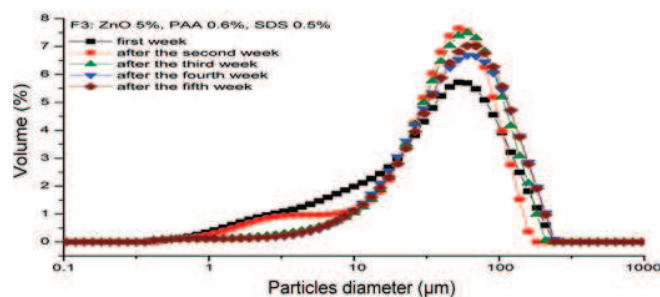
The backscattering profiles of F3 and F4 remain practically unchanged for the whole period of the analysis. For F9, a slight clarification is observed, but without sedimentation. Therefore, these formulations remain stable over time.

On the other hand, the formulas F1, F2, F5, F7 (initially stable) and F8, reveal a continuous variation of the profiles all along the sample during 15 days. Beyond the second week, the variation of the profiles is not significant, indicating that the recorded instabilities occur during the first two weeks.

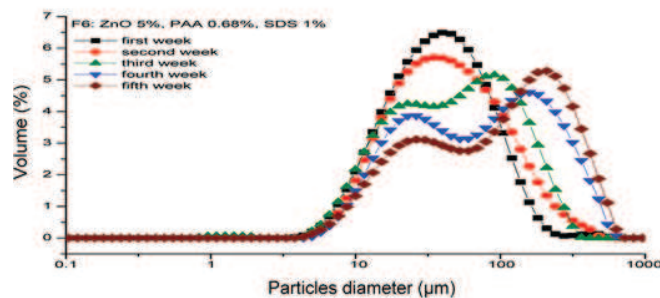
For F6, the increase of particle size induced by the destabilization phenomena (flocculation, coagulation), is



(a)



(b)



(c)

FIG. 7. Final particle size distribution (PSD) for the different formulations (a) and PSD versus time, for F3 (b) and F6 (c). (Color figure available online.)

easily identified by the Turbiscan ags (reduction of the backscattering intensity in the whole sample (Figure 9f). Beyond the second week, the profiles become reproducible. Moreover, the reproducibility of these profiles is not affected by the shift of the PSD toward larger size.

To study the influence of particle size on the backscattered intensity (so, on the destabilization phenomena observed for the majority of the formulations) and to understand the effect of the additive content on these phenomena, the profiles of the different formulations were compared (Figure 10). F1, F2, F5, and F8 present local variations of the backscattered intensity since the beginning of the analysis, meaning an early manifestation of instabilities. These variations are more significant for F5, which presents the highest level of backscattering intensity

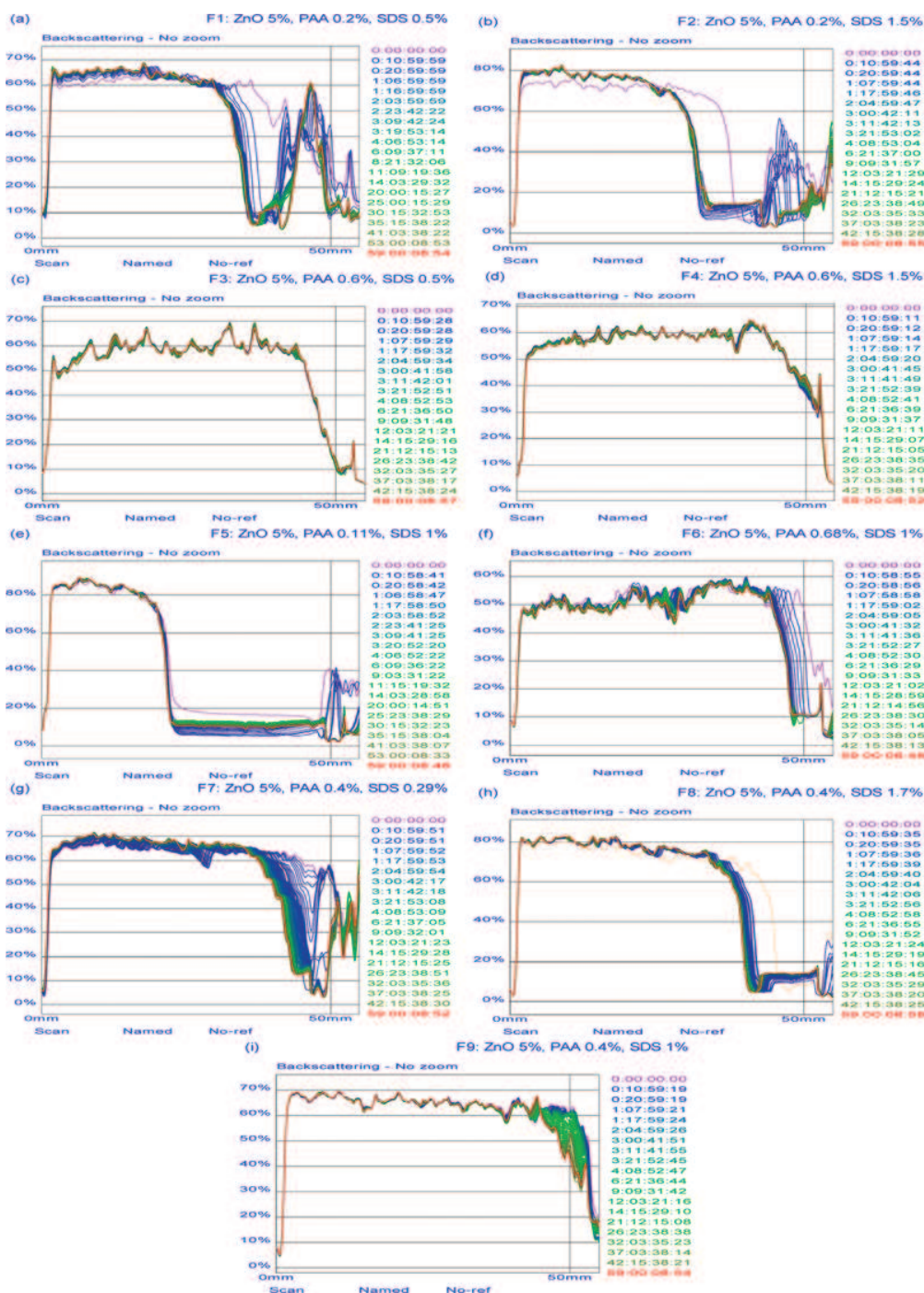


FIG. 8. Backscattered intensity profiles given by the Turbiscan ags, as a function of the height of the sample, and versus time, for the various formulations. (Color figure available online.)

at the bottom of the tube, indicating an extensive sedimentation, compared with F1, F2, and F8. The sedimentation rate of these formulations is directly related to their first PSD (Figure 6). The larger the particles size, the faster the sedimentation rate.

F3, F4, F6, F7, and F9, present uniform profiles, all along the sample, with relatively low backscattered intensities, showing that these formulations are fairly stable, at the beginning of the analysis. Also, for these formulations, the backscattered intensity is strongly correlated with the PSD.

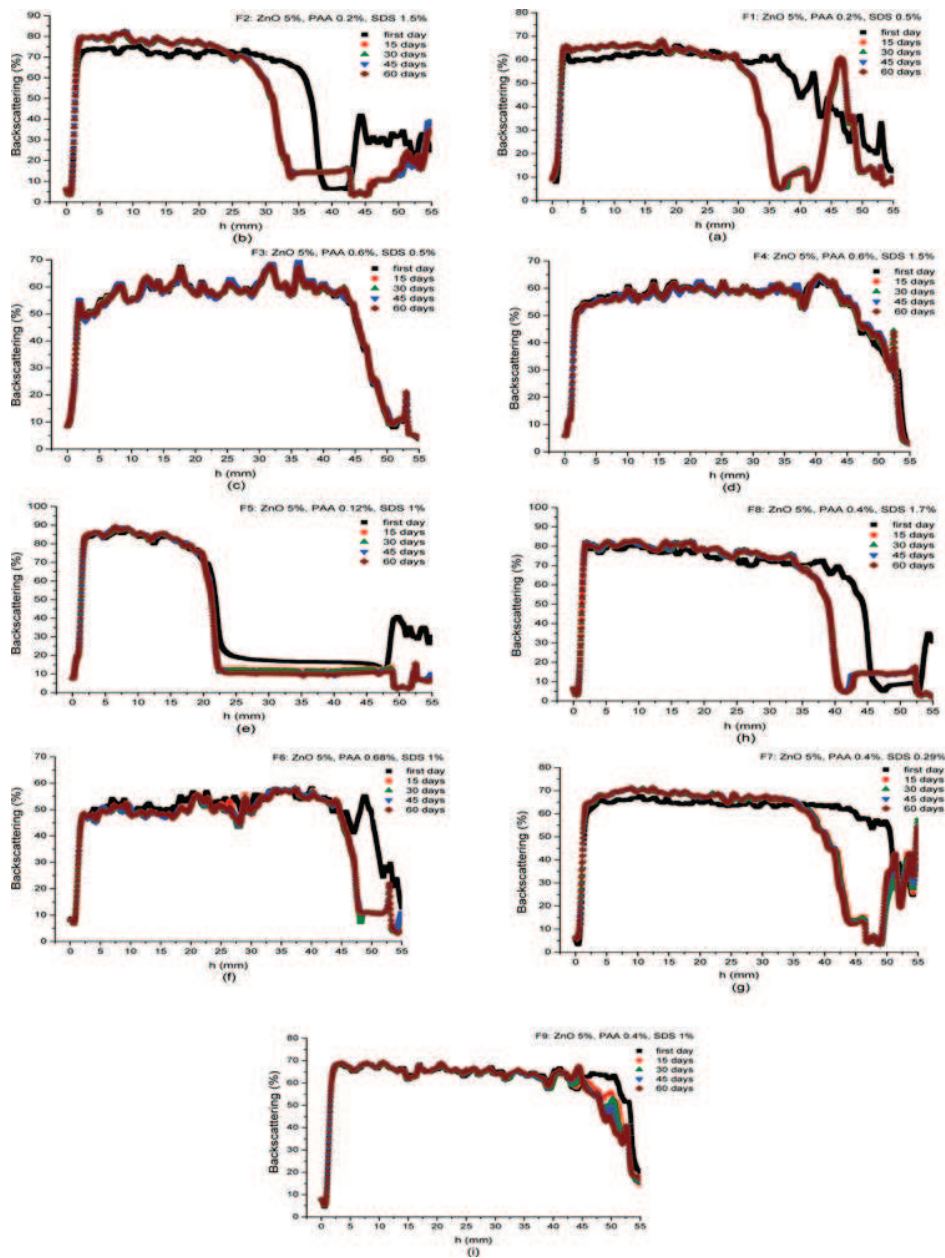


FIG. 9. Evolution of the destabilization phenomena, as a function of time, for the different formulations. (Color figure available online.)

The polymer has a preponderant effect on the backscattered intensity of our suspensions. At identical SDS content, the backscattered intensity at the bottom of the sample decreases (less formation of sediment) with an increase of the PAA concentration: therefore, the formulations containing higher proportions of polymer contain smaller size particles, are more viscous and more stable.

On the other hand, at identical PAA content (F1 compared with F2, F3 with F4, and F7 with F8 and F9), the suspensions containing higher SDS proportions give rise

to clarification at the top of the sample. Thus, they are less stable, in agreement with viscosity reduction by surfactant addition (fast physical destabilization of the suspension). Especially for the SDS-rich F8, flocculation is observed. Moreover, destabilized suspensions are not redispersible (redispersibility tests have been carried out).

ζ Potential

Measurements of ζ potential were carried out during the first weeks of storage. Let us recall that the ζ potential

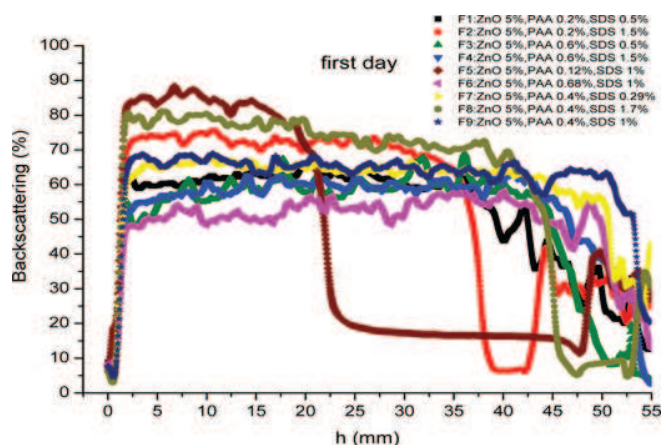


FIG. 10. Comparison of the backscattering profiles of the different formulations. (Color figure available online.)

measurements were carried out after centrifugation. Therefore, the measured ζ potential values are actually representative of the upper, clear colloidal phase of the sample. The experimental results, in absolute value, are given in Figure 11.

Stability is considered to be good when the ζ potential is higher than 60 mV in absolute value.

The ζ potential is strongly negative for the majority of our formulations and varies between -35 and -95 mV, corresponding to a zone of stability. It was already shown that the pH of our formulations only varies between 8 and 9, which enables them to remain in this zone of stability: the addition of polyacrylic acid should bring positive charges, but those are neutralized with NaOH and pH increases. When the isoelectric point is reached, the suspension is in its most unstable state. Alkalinization ($\text{pH} > 8$) brings back the suspension in a zone of stability.

We suppose that, more often, there is a relationship between the average size of the particles in the whole

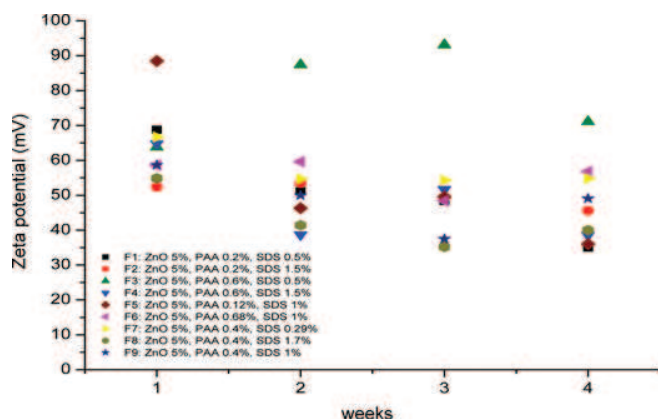


FIG. 11. ζ potential versus time for the various formulations. (Color figure available online.)

sample and in the supernatant. But the relationship between ζ potential and particle size is not straightforward. For example, F3 keeps the highest absolute values of ζ potential (from 63.8 to 93.1 mV) for the whole duration of the study: this confirms, once more, the remarkable stability of this formulation (small particles) compared with the others. On the other hand, F5, with lower absolute values of ζ potential, nevertheless belonging to the stability interval, seems to be stable only due to centrifugation.

Sedimentation/Clarification

Our suspensions are opaque and the determination of the height of sediment was not easy. For this reason, we preferred to represent the evolution of the clarification rate versus time. The results are shown in Figure 12.

Only the formulations F3, F4, and F9, containing 0.4 or 0.6% polymer, resisted sedimentation. The behavior of F6 (0.68% PAA, 1% SDS) deviates, once more, from that

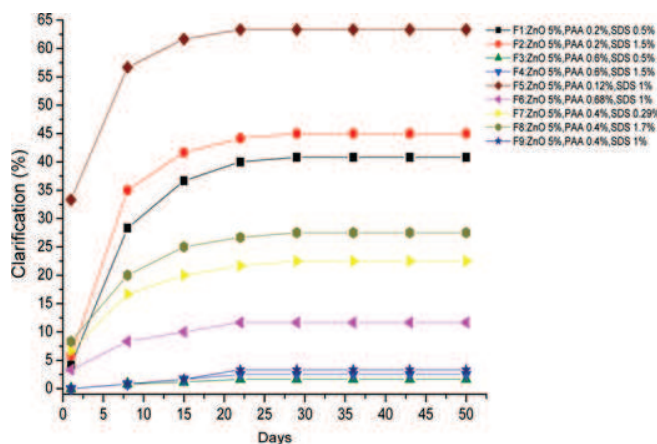


FIG. 12. Evolution of the clarification of the formulations as a function of time. The image shows the physical aspect of the “pure” suspension (5% ZnO) and of the various formulations after 8 weeks of storage. (Color figure available online.)

of the mixtures containing 0.6% of PAA (F3 and F4) and 1% of SDS (F9). For this formulation, the formation of a surface layer of continuous phase, containing some flocs in suspension and others which stick on the walls of the tube, is observed. The destabilization of the formulations F1, F2, F5, F6, F7, and F8 is initially fast, during the first two weeks of storage, then, strongly slows down thereafter. The first measurements indicate that F5 formed a deposit since the beginning of the test, with a clarification rate of 33%.

Figure 12 clearly shows that, after eight weeks of storage, the “pure” suspension (5% ZnO) did not resist sedimentation.

CONCLUSION

The control of the physical stability of ZnO suspensions, in the long run, is the principal objective of the present study. The presence of two phases (solid dispersed in a liquid) susceptible to separate by sedimentation or flocculation/coagulation, required techniques such as rheology, particle size measurements, multiple light scattering, and zetametry. In the linear viscoelastic domain ($<1\%$ strain), G' and G'' are very sensitive to additive (PAA and SDS) concentration. All the formulations present strong elastic properties for % strains lower than 10% ($G' > G''$ and $\tan \delta < 1$, associated particles). Beyond this deformation, a transition from the elastic to the viscous state was recorded. This transition, at low deformations, is an interesting and desirable characteristic since it simulates the facility of spreading of formulations on the skin. Consequently, the knowledge of these viscoelastic parameters can predict the performance of the products.^[17]

All the formulations show a shear-thinning behavior, a most desired property for pharmaceutical suspensions: an agitation of the bottle helps reduce the viscosity significantly and the product flows easily from the bottle. The polymer has a dominating effect on the rheological behavior of the suspensions. An increase of the PAA content raises the viscosity. The classical viscosity increase with particle size reduction seems well confirmed by our experimental results.

Multiple light scattering analysis, with the Turbiscan ags, supplements the rheological and particle size investigations and highlights the major role of the polymer on suspension stability.

In conclusion, the formulations prepared with higher proportions of polymer (0.4 and 0.6 wt%) contain smaller particles, are more viscous and remain stable and macroscopically homogeneous. Moreover, their homogeneity is not affected by the changes of particle size observed with the laser-light diffraction technique. pH and ζ potential measurements, as well as sedimentation tests still confirm the stability of these suspensions.

REFERENCES

- [1] Liufu, S.C., Xiao, H.N., and Li, Y.P. (2004) *Powder Technol.*, 145: 20–24.
- [2] Liufu, S.C., Xiao, H.N., and Li, Y.P. (2005) *Materials Letters*, 59: 3494–3497.
- [3] Tang, F.Q., Uchikoshi, T., and Sakka, Y. (2002) *J. Am. Ceram. Soc.*, 85: 2161–2165.
- [4] Usui, H., Shimizu, Y., Sasaki, T., and Koshizaki, N. (2005) *J. Phys. Chem. B*, 109: 120–124.
- [5] Zhang, L.L., Jiang, Y.H., Ding, Y.L., Povey, M., and York, D. (2007) *J. Nanoparticle Res.*, 9: 479–489.
- [6] Hiemenz, P.C. (1997) *Principles of Colloid and Surface Chemistry*; 3rd ed.; New York: Marcel Dekker.
- [7] Binner, J.G. P. and Davies, J. (2000) *J. Eur. Ceram. Soc.*, 20: 1539–1553.
- [8] Bhargava, H.N., Nicolai, D.W. and Oza, B.J. (1996) *Topical Suspensions in Pharmaceutical Dosage Forms, Disperse Systems*, vol. 2, edited by H.A. Lieberman, M.N. Rieger, and G.S. Banker; New York: Marcel Dekker, pp.193.
- [9] Evanko, C., Dzombak, D., and Novak, J. (1996) *Colloids Surf. A*, 110: 219–223.
- [10] Hidber, P., Graule, T. and Gauckler, L. (1997) *J. Eur. Ceram. Soc.*, 17: 239–249.
- [11] Hidber, P., Graule, T., and Gauckler, L. (1996) *J. Am. Ceram. Soc.*, 79: 1857–1867.
- [12] Baklouti, S., Romdhane, M., Boufi, S., Pagnoux, C., Chartier, T., and Baumard, J. (2003) *J. Eur. Ceram. Soc.*, 23: 906–911.
- [13] Falkiewicz, M.J. (1996) *Theory of Suspensions, in Pharmaceutical dosage forms, Disperse Systems*, vol. 1, edited by H.A. Lieberman, M.N. Rieger, and G.S. Banker; New York: Marcel Dekker.
- [14] Kibbe, A.H. (2000) *Handbook of Pharmaceutical Excipients*, 3rd ed; Washington, DC: American Pharmaceutical Association & Pharmaceutical Press.
- [15] Goddard, E.D. (1986) *Colloids and Surfaces*, 19: 301–329.
- [16] Binana-Limbele, W. and Zana, R. (1986) *Colloids and Surfaces*, 21: 483–494.
- [17] Iliopoulos, I., Wang, T.K., and Audebert, R. (1991) *Langmuir*, 7: 617–619.
- [18] Maltesh, C. and Somasundaran, P. (1992) *Colloids and Surfaces*, 69: 167–172.
- [19] Wang, C. and Tam, K.C. (2005) *J. Phys. Chem. B*, 109: 5156–5161
- [20] Mengual, O., Meunier, G., Cayré, I., Puech, K., and Snabre, P. (1999) *Talanta*, 50 (2): 445–456.
- [21] Yeong, S.K., Luckham, P.F., and Tadros, Th.F. (2004) *J. Colloid Interface Sci.*, 274: 285–293.
- [22] Adeyeye, M.C., Jain, A.C., Ghorab, M.K.M., and Reilly, W.J., Jr., (2002) *AAPS PharmSciTech*, 3 (2) Article 08.
- [23] Rohn, C.L. (1987) *J. Water-Borne Coatings*, 10 (3): 9, 12–17.
- [24] De Gennes, P.G. (1987) *Adv. Colloid Interface Sci.*, 27: 189–209.
- [25] Clasen, C. and Kulicke, W.M. (2001) *Prog. Polym. Sci.*, 26: 1839–1919.
- [26] Dunstan, D.E., Hill, E.K., and Wei, Y. (2004) *Polymer*, 45: 1261–1266.
- [27] Luckham, P.F. and Rossi, S. (1999) *Adv. Colloid Interface Sci.*, 82: 43–92.